FAST DIFFUSION BONDING TECHNIQUE FOR EXTRUSION-BASED ADDITIVE MANUFACTURING OF HIGH-STRENGTH ALUMINIUM ALLOYS

Sadettin Cem Altıparmak[1,2*] – Victoria A. Yardley[2] – Zhusheng Shi[2] – Jianguo Lin[2]

[1]Department of Applied Science and Technology, Politecnico di Torino, Corso Duca degli Abruzzi 24, 10129 Turin, Italy
[2]Department of Mechanical Engineering, Imperial College London, London SW7 2AZ, UK

ARTICLE INFO

***Article history*:**
Received:26.09.2024.
Received in revised form: 16.05.2025.
Accepted: 16.05.2025.

Keywords:
Keyword1
Keyword2
Keyword3

DOI: https://doi.org/10.30765/er.2657

Abstract

In aluminium and its alloys, the efficacy of diffusion bonding and extrusion-based additive manufacturing (AM) is greatly limited by the presence of aluminium oxide (Al2O3) on the surfaces to be bonded. In the present work, a novel fast diffusion bonding technique is introduced, in which the surfaces to be bonded are mechanically scraped using an abrasive file immediately before bonding to remove or break the surface Al2O3 layer and reduce surface roughness so that the holding time can be reduced. In the present work, the new fast diffusion bonding technique has been experimentally investigated by bonding similar half-dogbone specimens of aluminium alloys AA7075-T6 and AA6061 to determine the effects of the bonding temperature, bonding pressure and holding time on the strength and properties of the resulting bonded specimens. Bonding curves, showing the pressure required for successful bonding as a function of temperature and holding time, have been constructed. Using the novel technique has been found to increase the maximum strength in tension of bonded specimens of AA7075-T6 and AA6061 by around 12% and 11%, respectively, compared with the conventional method. Metallographic examination has shown that the novel technique aids in eliminating residual microvoids from the bonding interfaces, providing further evidence that the new technique is effective in promoting good-quality bonding. The present work has demonstrated the feasibility of the novel diffusion bonding technique and opens up the possibility for application of the technique in extrusion-based AM to give a hybrid-AM process, allowing high-quality bonding between successively printed layers.

1 Introduction

Additive manufacturing (AM), popularly known as 3D printing, offers greater design freedom than conventional fabrication techniques, allowing the manufacture of components with intricate geometries [1, 2]. Extrusion-based AM is a subcategory of AM technology, based on the physical state of raw AM materials, in which the material is extruded in a fluidlike form and deposited in successive layers to fabricate the desired geometry [3, 4]. As a result of its cost-effectiveness, relative simplicity and applicability to a large number of different classes of materials, particularly compared to liquid- and powder-based AM, extrusion-based AM has found application in a wide range of industrial sectors [4]. In extrusion-based AM, the feedstock material, which often consists of filaments, pellets or wires of a base material mixed with a polymeric binder to ease liquefaction, is heated to form a highly viscoelastic melt, which is forced out through nozzles in the print head

* Corresponding author
E-mail address: cem.altiparmak@polito.it

and deposited layer by layer [2]. The successively deposited layers solidify rapidly immediately after deposition. Adequate bonding between successive layers is necessary to ensure the integrity and soundness of the printed part [5]. In the current paper, the success in the experimental work was determined if a monolithic bonded specimen was extracted from the testing rig. Then, the bonding curves for AA7075-T6 and AA6061, showing the threshold bonding conditions to be applied for resulting in bonded joints, were generated based on the success achieved in the joints using the new diffusion bonding technique introduced in the study.

The bonding quality of diffusion-bonded specimens was analysed to evaluate the efficiency of the bonding technique. The assessment of the bonding quality was conducted based on several considerations using some techniques such as: (i) bonding strength results obtained in tensile testing, (ii) surface topography analysis of initial and fracture surfaces, (iii) microstructural investigation (i.e. surface morphology of initial and fracture surfaces), and (iv) existence of microvoids in the bonding interlayers and visual distinguishability of bonding lines under scanning electron microscopy. Mechanical scraping using an abrasive file, with application of pressure, is used to rupture or remove the oxide layer and thereby reduce the roughness of the surfaces to be bonded. The purpose of this is to reduce the holding time required for the closure of microvoids, i.e. the voids formed when the bonding surfaces are brought into physical contact, and therefore for the formation of a sound bond. The present paper gives details of the new diffusion bonding technique and of diffusion bonding experiments, carried out using a purpose-built rig, to determine appropriate process parameters (bonding pressure, bonding temperature and holding time) and the efficacy of mechanical removal of bonding surfaces. Tensile test results on the resulting diffusion-bonded specimens and microscopic investigations on selected fractographic and polished specimens are used to show the efficacy of applying the new technique and the improvement in the properties of bonds with respect to those obtained using a conventional diffusion bonding technique without abrasive scraping. The results of the present study can be used to implement the new technique in a hybrid-AM process in future work.

2 Experimental Methods

2.1 Principle of Fast Diffusion Bonding Technique

While the novel diffusion bonding technique is expected to be of great utility in itself, one aim of its development is to provide insight into the feasibility and optimal values of bonding parameters in a proposed hybrid-AM technique for the improvement of bond quality in aluminium alloys. This hybrid process comprising the novel diffusion bonding technique would consist of material deposition of each layer via extrusion-based AM followed by mechanical scraping of the surfaces and then rolling with a plastic deformation of around 5% for a time of the order of 10 seconds. Since the proposed hybrid-AM process involves the application of stress to a material that is cooling from high temperature, the bonding mechanism is likely to be similar to that in solid-state joining techniques such as diffusion bonding. In this new technique, a 316 stainless steel file of thickness 1 mm coated with an abrasive layer comprising 1000 grit cubic boron nitride diamond is used to mechanically scrape the bonding surface of the aluminium alloy immediately before diffusion bonding. The scraping pressure is a vertical pressure applied while the abrasive file is dragged laterally across the bonding surfaces. The optimised scraping pressure of 1 MPa obtained using this procedure was set in the commercially available software platform Cubus 2.1.69 for application during the process.

2.2 Materials and Process Parameters

The as-received materials were machined using a high-speed CNC machine to obtain half-dogbone specimens, whose geometry and dimensions are shown in Figure 1(a). These specimens were diffusion bonded to form complete tensile test specimen whose dimensions before diffusion bonding are given in Figure 1(b). The abrasive files used in the study to scrape the bonding surfaces were designed in-house and produced by Cranden Diamond Products Ltd. They consist of a 316L stainless steel holder and shank, with a 1000 grit cubic boron nitride diamond abrasive layer of thickness 1 mm. The abrasive sections of the upper and lower surface of the files were electroplated with nickel to prevent the adhesion of aluminium alloy to the abrasive surface, and thereby to give good resistance to corrosion and wear [8]. The abrasive file in use was periodically exchanged with a new file when it was determined, by visual inspection, that the abrasive surfaces had become excessively contaminated by material, mainly aluminium.

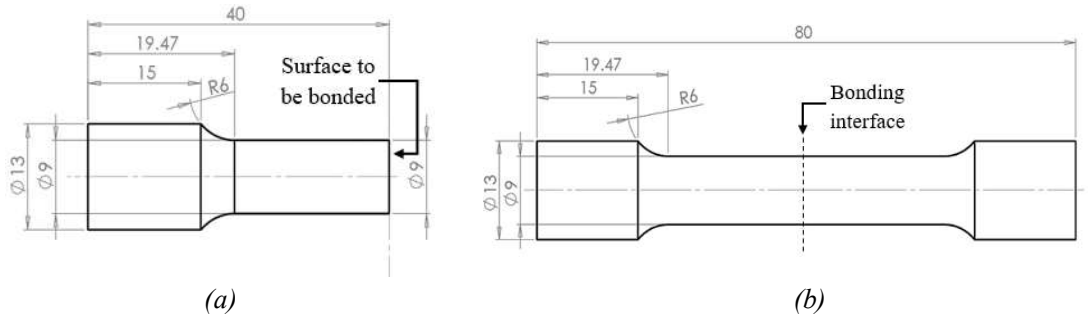

Figure 1. Dimensions of aluminium alloy specimens: (a) half-dogbone specimen before diffusion bonding, and (b) arrangement of two half-specimens brought into physical contact before diffusion bonding (all dimensions are in mm).

Diffusion bonding experiments were conducted at three different temperatures, i.e. 450°C, 475°C, and 500°C, which were selected to replicate typical temperatures used to liquefy aluminium alloys and thereby facilitate deposition in extrusion-based AM. The full set of conditions of temperature, bonding pressure and holding time used in the diffusion bonding experiments conducted for specimens to be used in tensile testing and microstructural analysis are given in Table 1 for AA7075-T6 and AA6061. The upper limit of bonding pressure for each temperature was taken to be the maximum true stress value corresponding to a strain rate of 0.1 s-1 on the compressive true stress-strain curves for AA7075-T6 and AA6061, and given in [9] and [10] respectively. Such upper limits are necessary to avoid subjecting the materials to excessive plastic deformation (EPD). This, which is caused by excessive bonding pressure applied in the normal direction to the bonding interfaces, leads to reduction in height in the compression direction together with lateral slip and unacceptable shape distortion.

2.3 Equipment and Experimental Procedure

Figure 2 is a photograph of the test rig for fast diffusion bonding experiments assembled within an Instron laboratory furnace. This resistance heating furnace has holes of diameter 65 mm in its top and bottom to accommodate the upper and lower punches that will compress the specimens. Both upper and lower punches are fabricated from 316L stainless steel. The lower punch was an off-the-shelf component of height 300 mm and diameter 55 mm, and the upper punch was supplied as a bar of height 750 mm and diameter 55 mm by N H Global Ltd, UK, and CNC cut and machined in-house to a height of 550 mm and a diameter of 50 mm. The upper punch was then threaded with a thread angle of 60°, a pitch of 1.25 mm, and a depth of 2.7 mm in order to enable it to be screwed into a load cell of capacity 250 kN located above the rig and laboratory furnace, as shown in Figure 2(a). The temperature of the specimens being bonded was continuously measured using a thermocouple wire attached to the lower specimen using a fire-resistant band, and connected to an off-the-shelf 307P Staitech J-type digital thermocouple. The furnace was positioned at the base of an ESH biaxial 250kN hydraulic press (Figure 2(b)). The displacement of the upper punch was controlled using Cubus 2.1.69 software, and the load applied by the upper punch directly to the upper specimen was controlled by the load cell, also using the Cubus software. Note that the pressure applied during bonding was only in the vertical (normal) axis, giving a uniaxial stress state since there were no lateral constraints on the specimens.

Table 1. Conditions used in diffusion bonding experiments for AA7075-T6 and AA6061: holding times (in seconds) for different bonding temperatures and pressures (bold type = both tensile testing and surface morphology analysis, italic type = microstructural investigation, with asterisks = repeat test specimens produced with and without using abrasive file, and the rest = only used in mechanical testing).

Bonding pressure (MPa) / Bonding temperature (°C)	10	12.5	13.75	15	20	22.5	25	27.5	30	35	40	42.5	45
AA7075-T6 450	–	–	–	30	10, 30	–	10	10	7.5, **10**	7.5, *10*	5, 7.5	5	5, 7.5
AA7075-T6 475	30	30	–	10, 30	10	–	10	**10**	5, 7.5, **10** **30**	*10*	2.5, 5, *10*	2.5	2.5, 5
AA7075-T6 500	30	10, 30	30	5, 10	5, 10*	5	5, 7.5, *30*	5, 7.5	–	5	5	–	–

Bonding pressure (MPa) / Bonding temperature (°C)	1.25	2.5	4.5	5	7.5	10	12.5	15	17.5	20	25	30	35
AA6061 450	–	3.5	–	2.75, **3.5**, *5*	–	2	–	2	–	1.5, 2	–	1.25, 1.5	1.5
AA6061 475	–	2.75, 5	2.75, 5*	2, 2.75, 10	2	2	–	1.5, *2*, *5*	–	1.5	1.25, 1.5	1.5	–
AA6061 500	1	0.5, 1	–	0.5	0.25, *0.5*, 1, *1.5*	–	0.25	0.125, 0.25	0.125	–	–	–	–

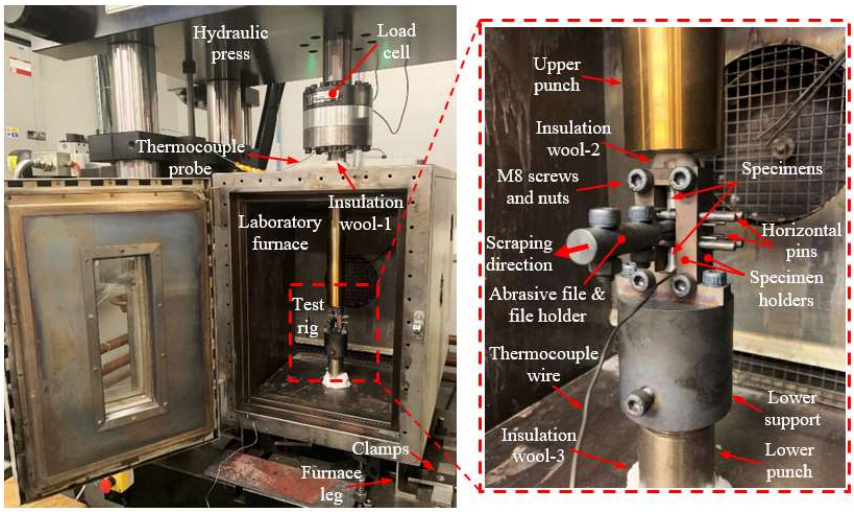

(a) *(b)*

Figure 2. Equipment for experimental diffusion bonding technique.

2.4 Mechanical Testing and Metallography on Diffusion-Bonded Specimens

The effect of the bonding parameters on the soundness of the bonds in the AA7075-T6 and AA6061 specimens was investigated using tensile testing. This was carried out using a universal 10kN load capacity Instron 3366 tensile testing machine equipped with the commercially available Bluehill 3 software. A relatively low extension rate (i.e. crosshead speed, tensile testing speed) of 0.2 mm/min was used to enable testing of specimens that were successfully bonded, but had been subjected to lower values of bonding pressure, temperature and/or holding time, and were therefore delicate and prone to failure. The specimens, which have circular-section ends, were held in custom-designed circular grips. An increasing uniaxial tensile load was applied until failure occurred. Fractography was carried out on the surfaces of the failed tensile specimens of AA7075-T6 and AA6061 using a TESCAN MIRA scanning electron microscope (SEM) in SE mode with an accelerating voltage of 25 keV and a beam current of 3 nA at magnifications of 50x, 100x, 1000x and 1700x. Specimens were prepared by cutting, mounting, grinding and polishing. The roughness of the AA7075-T6 and AA6061 bonding surfaces before diffusion bonding was measured using a Bruker Contour GT 3D optical microscope. The surface roughness Ra, which is the mean deviation of peaks or valleys from the line of mean height, was measured by analysing the whole bonding surface. SEM images of the surfaces were also taken using a TESCAN MIRA scanning electron microscope (SEM) in SE mode using an accelerating voltage of 25 keV and a beam current of 3 nA at a magnification of 50x.

3 Results and discussion

Figure 3(a) shows an SEM image of the whole bonding surface of AA7075-T6. Figure 3(b) is a surface topography image, taken using the Bruker 3D optical microscope, of a rectangular area centred on the centre of the AA7075-T6 specimen, as indicated with white dashed lines in Figure 3(a), and Figure 3(c) is an equivalent image for the AA6061 specimen. The two topographic images show that the asperities are equally spaced in the radial direction and their heights are all very similar thanks to the high-speed CNC surface finish. The surface roughness values, Ra, of the initial AA7075-T6 and AA6061 bonding surfaces are 0.716 μm and 0.709 μm respectively.

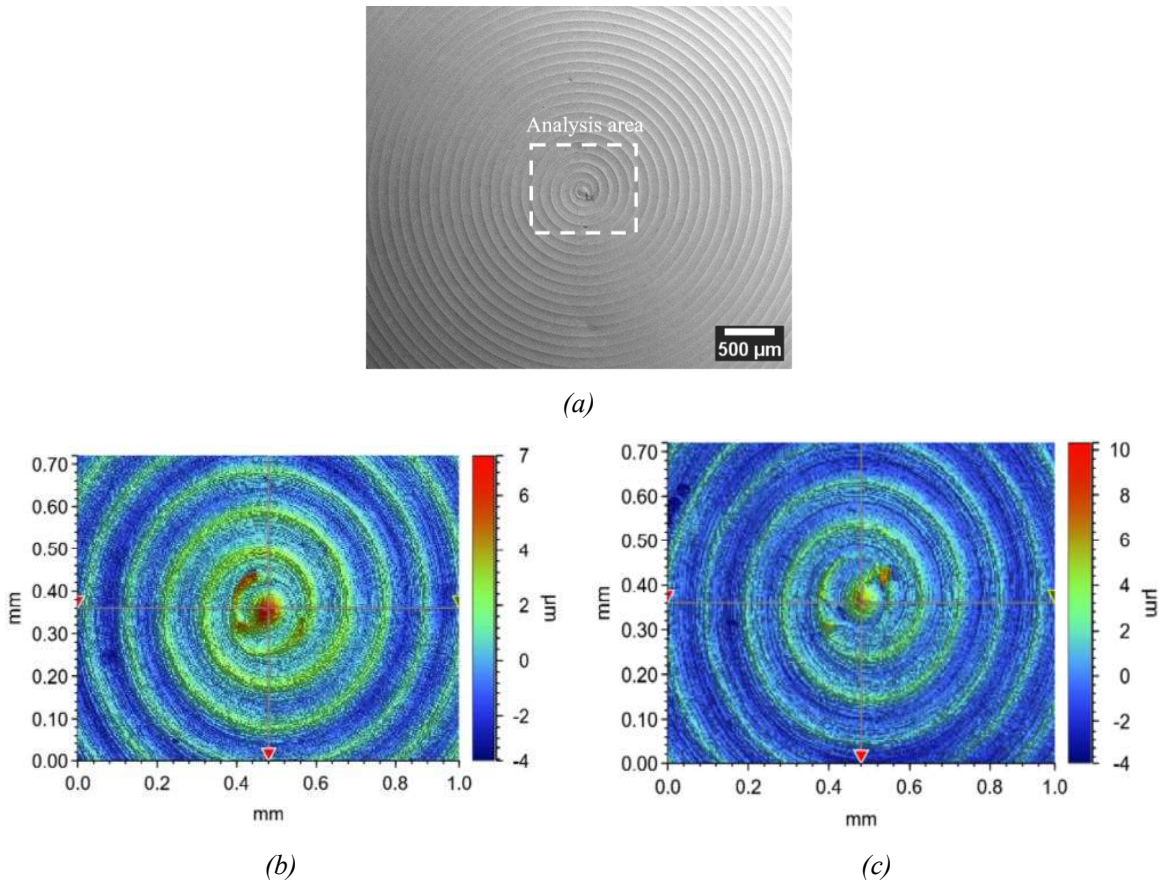

Figure 3. 2D Surface profiles of the initial surface of AA7075-T6 and AA6061: (a) SEM image of the bonding surface and central region where surface roughness analysis was performed, and (b, c) surface topography images of the central region of specimens of AA7075-T6 and AA6061 respectively.

3.1 Bonding Curves

Bonding curves are 2D diagrams indicating the minimum values of the parameters (bonding temperature, bonding pressure and holding time) that allow successful bonding. Success, in this context, is defined as the production of a monolithic dogbone specimen which had a strength value recorded before failure when tested in tension. If two independent half-dogbone specimens were still present after extraction from the sample holders following the diffusion bonding experiment, bonding was considered unsuccessful. The bond strengths of the successfully diffusion-bonded specimens are shown in the bonding curves in Sections 3.3.1 and 3.3.2. All the results presented in the rest of Section 3 are for specimens bonded using the new fast diffusion bonding technique, apart from those obtained for comparison using the conventional diffusion bonding technique, i.e. without use of the abrasive file, under bonding conditions of AA7075-T6-500°C-20MPa-10s (Figure 4(c)) and AA6061-475°C-5MPa-5s (Figure 4(b)). Individual bonding curves (for the single bonding temperatures 450°C, 475°C and 500°C), and combined bonding curves comprising curves for all three temperatures, were generated for all bonded specimens. In these curves, cross symbols (positioned exactly at the data point) are used to represent unsuccessful bonding, and tick symbols (positioned exactly at the data point) to represent successful bonding. Certain specimens underwent excessive plastic deformation (EPD) as a result of excessive bonding pressures; these cases, in which the experiments were arrested to avoid damage to the equipment, are indicated with diagonal hatching in the individual bonding curves given in Figure 4(a-c) and Figure 5(a-c). The individual curves were generated by connecting data points representing the minimum values of the bonding parameters needed to achieve a successful bond, as defined above. The combined curves show the individual curves together without indicating the limit data points for easier comparison.

3.2 Bonding Curves for AA7075-T6 and AA6061

Figure 4(a-c) shows the individual bonding curves for AA7075-T6 at the three different diffusion bonding temperatures; the combined bonding curves for this alloy are given in Figure 4(d). The bonding pressure values above which excessive plastic deformation was observed were 42.5 MPa, 41.5 MPa and 26 MPa at 450°C, 475°C and 500°C respectively. Comparison of the individual bonding curves for AA7075-T6 at the three temperatures shows that the shape of the curves is similar for all temperatures. It can be seen from the combined curves shown in Figure 4(d) that, for a given holding time, successful bonding was achieved at lower bonding pressures when the temperature was higher. This can be attributed to the combined effect of lower hardness and higher diffusion coefficient at higher temperatures, enabling plastic deformation of surface asperities and creep-assisted closure of microvoids at lower pressures.

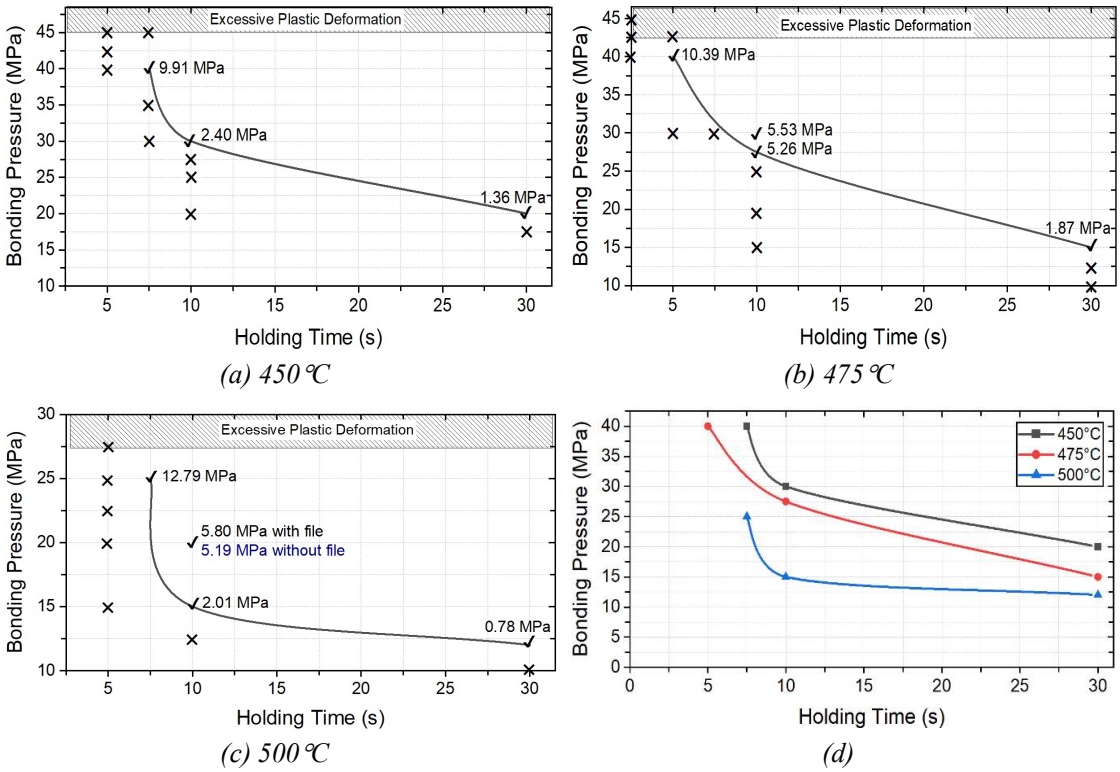

Figure 4. Individual bonding curves for AA7075-T6 generated for: (a) 450°C, (b) 475°C, (c) 500°C, and (d) combined bonding curves for AA7075-T6 (bonding strength values are indicated).

The individual and combined bonding curves of AA6061 generated for the three different diffusion bonding temperatures 450°C, 475°C and 500°C are plotted in Figure 5. These curves show a similar trend to those of AA7075-T6, namely that the higher the bonding temperature, the shorter the time required to achieve successful bonding. However, when comparing Figure 4(d) and Figure 5(d), it can be seen that successful bonding was attained at lower bonding pressures and in shorter holding times in AA6061 than in AA7075-T6 (note, particularly, the difference in x-axis scaling between these two figures). In AA6061, the limiting pressures above which EPD occurred were 32 MPa, 27 MPa and 16 MPa for bonding temperatures of 450°C, 475°C and 500°C respectively. Note that such pressure values, particularly those above 15 MPa, are significantly higher than the pressures normally associated with diffusion bonding (around 1.25-5 MPa); instead, these values are similar to those used in pressure welding. The reason for carrying out diffusion bonding experiments at such high pressures is that there is a lack of data in the literature on the effect of using such pressures and how this might affect bonding behaviour in the proposed hybrid-AM process. The highest bond strength, measuring 34.78 MPa, was achieved on the bonding curves among all diffusion-bonded specimens with AA6061 alloy bonded at 475°C-25MPa-1.5s, subsequent to abrasively scraping the bonding

surfaces. In AA6061, in contrast to AA7075-T6, there is a significant difference between the two bonding curves for 450°C and 475°C, and that for 500°C, namely a large shift of the limit bonding curve towards smaller values of pressure and holding time.

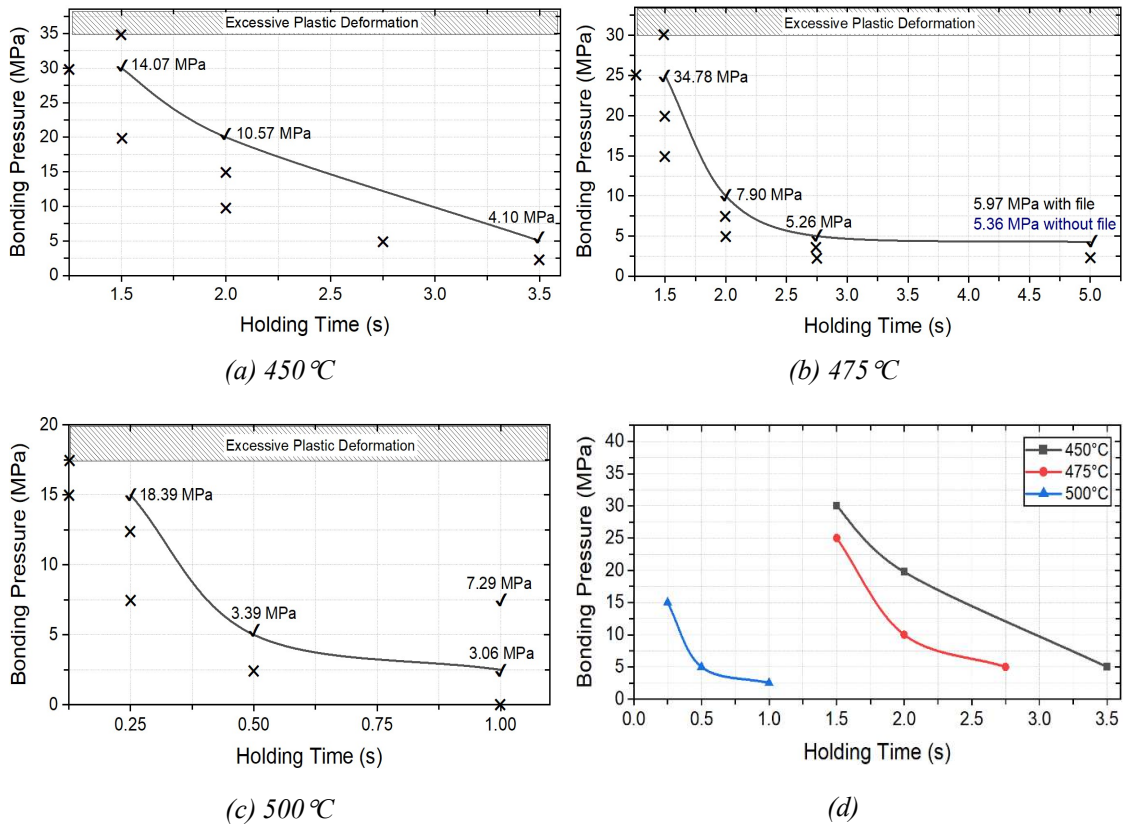

Figure 5. Individual bonding curves for AA6061 generated for: (a) 450°C, (b) 475°C, (c) 500°C, and (d) combined bonding curves for AA6061 (bonding strength values are indicated).

Figure 4(a-c) also gives the numerical values of bond strength (maximum strength value recorded before failure) for AA7075-T6 specimens produced using the new fast diffusion bonding technique and Figure 5(a-c) the results for AA6061. From these figures it is evident that higher bond strengths were obtained at higher temperatures for the same bonding pressure and holding time. For instance, the tensile strength of AA7075-T6-30MPa-10s at 450°C was more than double, at 5.53 MPa, that of the same alloy bonded with otherwise the same bonding parameters but at 475°C, i.e. 2.40 MPa. A further increase in the bonding temperature, to 500°C, gave an even larger increase in the bond strength in both alloys. For example, comparing Figure 4(b, c), it can be seen that the bond strength of the AA7075-T6 specimen bonded under conditions of 500°C-15MPa-10s was higher (2.01 MPa, Figure 4(b)) than that achieved, i.e. 1.87 MPa after applying the same bonding pressure of 15 MPa at 475°C, even after a holding time three times longer (Figure 4(c)). Bond strengths of diffusion-bonded specimens produced without using the abrasive file for comparison are presented in Figure 4(c), for the specimen AA7075-T6-500°C-20MPa-10s and Figure 5(b), for the specimen AA6061-475°C-4.5MPa-5s. In the AA7075-T6 specimen, a bond strength of 5.19 MPa was obtained without the abrasive file, as compared to 5.80 MPa (i.e. 12% higher) obtained under the same conditions with the abrasive file. In AA6061 (Figure 5(b)), the bond strength obtained was 5.36 MPa when the abrasive file was not used, and 5.97 MPa when it was used (i.e. an increase of 11%). These results show that a demonstrable benefit in increased bond strength is obtained when the new fast diffusion bonding technique is used.

3.3 Microscopic Investigation of AA7075-T6 and AA6061 Joins

This section details the microscopy investigation results based on the comparison between the initial (prior to bonding) and fracture surfaces (after failing under tensile testing) of successfully bonded some AA7075-T6 and AA6061 specimens in Figure 4 and Figure 5 indicated with tick symbols. Figure 6 presents SEM micrographs showing the effect of different bonding conditions on the surface morphology in AA7075-T6. Figure 6(a) shows the initial surface of AA7075-T6 before diffusion bonding (50x); the spiral morphology introduced by the cutter of the CNC machine can clearly be seen. Figure 6(b) shows the fracture surface, after tensile testing, of AA7075-T6 diffusion bonded successfully at 475°C-40MPa-5s (50x) and (c) the fracture surface of specimens bonded at 500°C-15MPa for 30 s. It can be seen that the morphology of the fracture surfaces depends strongly on the diffusion bonding parameters applied. In particular, the spiral morphology and traces of the scraping carried out by the abrasive file can still be seen in Figure 6(b) after bonding and fracture. The spiral morphology has been almost completely obliterated in Figure 6(c), corresponding to a holding time of 30 s (bonding surfaces were scraped at 45°). It can be inferred from these two examples that increasing the holding time has led to increased crushing of the surface asperities originally introduced by the cutter of the CNC machine.

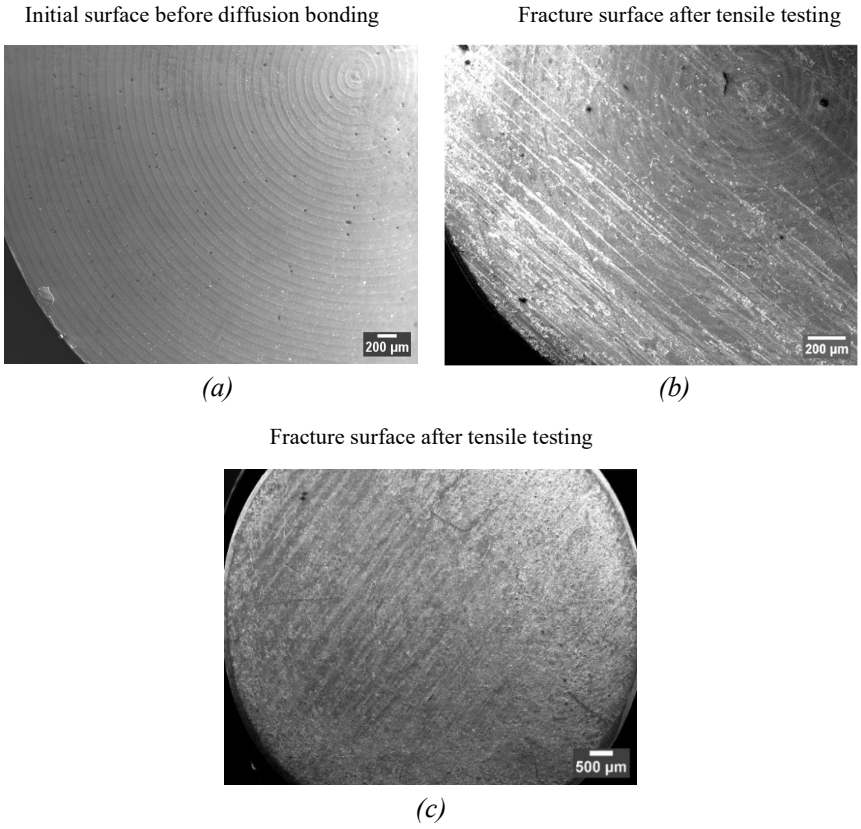

Figure 6. SEM micrographs of: (a) initial surface of AA7075-T6, (b) fracture surface of AA7075-T6 diffusion bonded at 475°C-40MPa-5s after tensile testing, and (c) fracture surfaces of AA7075-T6 diffusion bonded at 500°C-15MPa for holding time of 30 s.

3.4 Microstructural Investigation of Bonding Interfaces

Figure 7 shows the bonding interface area in AA6061 diffusion bonded at 475°C-15MPa-2s without scraping with the abrasive file (Figure 7(a)) and with the file (Figure 7(b)). These conditions should be within the successful bonding range if the abrasive file is used, according to the bonding curves in Figure 6(b). The bonding interface of AA6061 without scraping (Figure 7(a)) is broadly similar in appearance to that of AA7075-T6. Two microvoids are visible in the bonding interface in Figure 7(a) and, on the basis of this micrograph, these appear wider than those in AA7075-T6. The use of an abrasive file for AA6061, with

otherwise the same bonding conditions (Figure 7(b)) resulted in an indistinguishable bonding line with no visible microvoids, suggesting that in this alloy, as in AA7075-T6, the scraping of bonding surfaces prior to bonding promotes the closure of microvoids in the bonding interfaces.

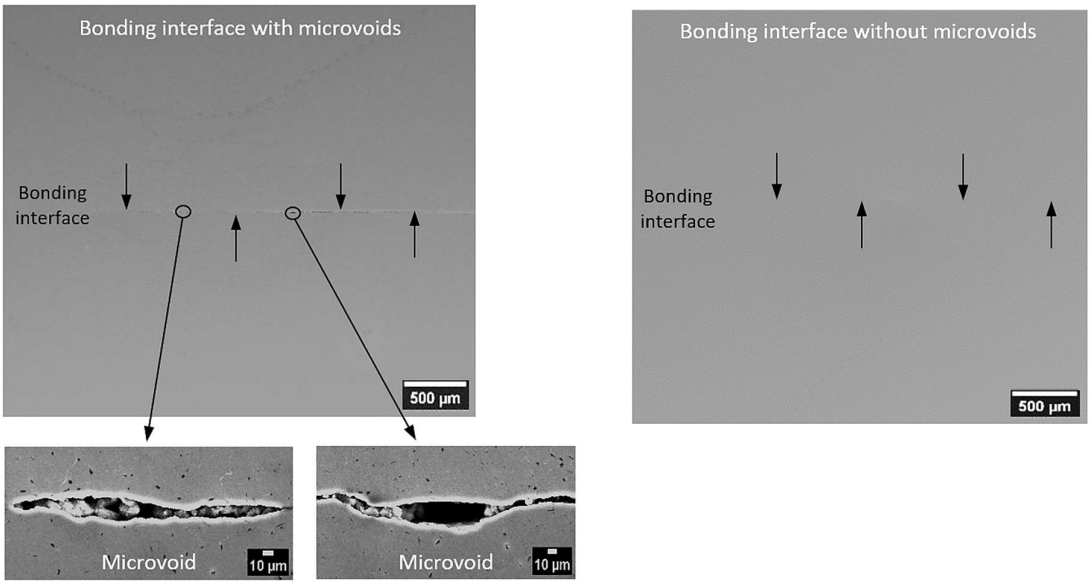

Figure 7. Bonding interface area in AA6061 diffusion bonded at 475°C-15MPa-2s: (a) without, and (b) with abrasive file to scrape bonding surfaces.

The present study has demonstrated beneficial results in aluminium alloys with the new fast diffusion bonding technique. After testing to determine optimal operating conditions, the new technique could be combined with extrusion-based AM processes to give a hybrid-AM process that would increase the strength of bonds between successively deposited aluminium alloy layers. The threshold bonding conditions are indicated on the bonding curves generated for AA7075-T6 and AA6061. It is recommended to apply at least the bonding conditions indicated on these curves in diffusion bonding and extrusion-based AM applications to achieve aluminium alloy joints bonded at temperatures of 450°C, 475°C, and 500°C, thus avoiding unsuccessful experiments resulting from the failure in the bonding of base materials. Additionally, bonding conditions located as far as possible towards the upper right of bonding curves are suggested to be applied in the applications to achieve higher bonding strength for more sound bonded joints and parts.

4 Conclusions

The present study has proposed a new, fast diffusion bonding technique for aluminium alloys, in which bonding pressures and temperatures are applied for shorter holding times, i.e. 0.25 to 30 seconds, than are used in conventional diffusion bonding techniques, namely 30 minutes [11] to 6 hours [12]. In the new technique, the surfaces to be bonded are scraped using an abrasive file to mechanically remove or rupture the naturally formed Al2O3 on the bonding surfaces. Diffusion bonding experiments have been conducted on similar AA7075-T6 and AA6061 alloy pairs to investigate the effect of varying the diffusion bonding parameters on the bond strength of the resulting specimens, which is defined as the strength value recorded before failure. Tensile test results on these specimens have been used to construct temperature-pressure-time bonding curves showing the minimum conditions required for successful bonding in AA7075-T6 and AA6061. The nature of the bonds obtained using the new technique has been further evaluated microscopically in terms of: (i) the surface morphology of fracture and initial bonding surfaces, (ii) the presence of residual microvoids in the bonding interfaces, and (iii) the visibility (distinguishability) of bonding lines. The main conclusions drawn from the paper can be summarised as follows:

- The mechanical scraping of bonding surfaces using abrasive files increased the strength of bonds between similar aluminium alloy pairs compared to those obtained under otherwise the same conditions without

mechanical scraping. For instance, the bond strength achieved with mechanical scraping was around 12% greater in the AA7075-T6 sample bonded at 500°C-20MPa-10s and 11% greater in the AA6061 sample bonded at 475°C-5MPa-5s. No residual microvoids were present in the interfacial region of the specimens bonded using the abrasive files. This was attributed to a decrease in the initial surface roughness resulting from scraping these bonding surfaces before application of bonding pressure.

- Excessive plastic deformation occurs when the bonding pressure is greater than an upper limit value which depends on the material and temperature. It is essential that the bonding pressure be lower than this upper limit to avoid the unacceptable dimensional change that can result from excessive plastic deformation.

- The bond strength of AA7075-T6 and AA6061 specimens increased as a result of an increase in any of the diffusion bonding parameters investigated (i.e. bonding temperature, bonding pressure and holding time). The highest bond strength of all diffusion-bonded specimens, i.e. 34.78 MPa, given on the bonding curves was obtained in AA6061 diffusion-bonded at 475°C-25MPa-1.5s after scraping of the bonding surfaces using the abrasive file.

References

[1] J. Gardan, "Additive manufacturing technologies: state of the art and trends," Int. J. Prod. Res., vol. 54, no. 10, pp. 3118–3132, 2016, doi: 10.1080/00207543.2015.1115909.

[2] I. Gibson, D. Rosen, and S. Brent, Additive Manufacturing Technologies: 3D Printing, Rapid Prototyping, and Direct Digital Manufacturing, 2nd ed. New York: Springer, 2015.

[3] K. Rane and M. Strano, "A comprehensive review of extrusion-based additive manufacturing processes for rapid production of metallic and ceramic parts," Adv. Manuf., vol. 7, no. 2, pp. 155–173, 2019, doi: 10.1007/s40436-018-00239-0.

[4] S. C. Altıparmak, V. A. Yardley, Z. Shi, and J. Lin, "Extrusion-based additive manufacturing technologies: state of the art and future perspectives," J. Manuf. Processes, vol. 83, pp. 607–636, 2022, doi: 10.1016/j.jmapro.2022.09.002.

[5] J. Blindheim, Ø. Grong, T. Welo, et al., "On the mechanical integrity of AA6082 3D structures deposited by hybrid metal extrusion & bonding additive manufacturing," J. Mater. Process. Technol., vol. 282, 2020, doi: 10.1016/j.jmatprotec.2020.116695.

[6] R. Braun, "Effect of thermal exposure on the microstructure, tensile properties and the corrosion behaviour of 6061 aluminium alloy sheet," Mater. Corros.-Werkst. Korros., vol. 56, no. 4, p. 243, 2005, doi: 10.1002/maco.200503927.

[7] D. Q. Zhang, J. Li, H. G. Joo, et al., "Corrosion properties of Nd
laser-GMA hybrid welded AA6061 Al alloy and its microstructure," Corros. Sci., vol. 51, no. 6, pp. 1399–1404, 2009, doi: 10.1016/j.corsci.2009.03.010.

[8] W. Sha, X. Wu, and K. G. Keong, "Applications of electroless nickel–phosphorus (Ni–P) plating," in Electroless Copper and Nickel–Phosphorus Plating, 1st ed., 2011, pp. 263–274, doi: 10.1016/B978-0-08-096496-0.00011-3.

[9] A. Jenab, A. K. Taheri, and K. Jenab, "The use of ANN to predict the hot deformation behavior of AA7075 at low strain rates," J. Mater. Eng. Perform., vol. 22, no. 3, pp. 903–910, 2013, doi: 10.1007/s11665-012-0376-2.

[10] S. S. Ding, Q. Y. Shi, and G. Q. Chen, "Flow stress of 6061 aluminum alloy at typical temperatures during friction stir welding based on hot compression tests," Metals, vol. 11, no. 5, p. 804, 2021, doi: 10.3390/met11050804.

[11] H. Y. Wu, S. Lee, and Y. H. You, "Genuine solid-state bonding characteristics of superplastic Al-alloys," J. Mater. Process. Technol., vol. 122, no. 2-3, pp. 226–231, 2002, doi: 10.1016/S0924-0136(02)00060-3.

[12] Y. Huang, N. Ridley, F. J. Humphreys, et al., "Diffusion bonding of superplastic 7075 aluminium alloy," Mater. Sci. Eng. A, vol. 266, no. 1-2, pp. 295–302, 1999, doi: 10.1016/S0921-5093(99)00092-6.